Infrared semiconductor laser modules for DIRCM applications

J. Wagner[a], S. Hugger[a], B. Rösener[a], F. Fuchs[a], M. Rattunde[a], Q. Yang[a], W. Bronner[a], R. Aidam[a], K. Köhler[a], M. Raab[b], E. Romasew[b], H. D. Tholl[b]

[a]Fraunhofer-Institut für Angewandte Festkörperphysik (IAF), Tullastrasse 72, 79108 Freiburg, Germany

[b]Diehl BGT Defence, Alte Nussdorfer Strasse 13, 88662 Überlingen, Germany

ABSTRACT

We report on the concept, realization and performance data of infrared semiconductor laser modules serving as compact and robust laser sources for a Directed Infrared Countermeasures (DIRCM) system. While the 2-2.5 µm atmospheric transmission window is covered by a GaSb-based optically pumped semiconductor disk laser (OPSDL), delivering a continuous-wave (cw) or temporally modulated output of ≥ 1 W with a high beam quality ($M^2 < 3$), an external cavity (EC) quantum cascade (QC) laser module is used to cover the 4.5-5 µm spectral range. The EC-QC laser concept allows efficient spectral beam combining of the output of several QC laser located side-by-side on the same semiconductor chip, while preserving the high-quality output beam of a single emitter. Both the OPSDL and the EC-QC laser have been integrated into rugged laser modules, comprising also all necessary power supply and control electronics, ready for use in field trials.

Keywords: Infrared semiconductor lasers, infrared laser modules, directed infrared countermeasures (DIRCM), quantum cascade laser, QC laser, optically pumped semiconductor disk laser (OPSDL), vertical-external-cavity surface-emitting laser (VECSEL), spectral beam combining

1. INTRODUCTION

Directed infrared countermeasure (DIRCM) systems, capable of injecting false information into the tracking sensor of a heat-seeking missile, require mid-infrared laser sources emitting in the 2-5 µm spectral range with an average output power exceeding 1 W and, at the same time, a high beam quality (beam propagation factor $M^2<3$) [1]. Furthermore, for deception class DIRCM the laser source has to be modulated in intensity with a high on/off contrast ratio at frequencies > 10 kHz [1].

As discussed in detail in, e.g., Ref. [2], the 2-2.5 µm spectral window can be covered by a GaSb-based optically pumped semiconductor disk laser (OPSDL), capable of producing a multiple-Watt output power in a high quality ($1.1 \leq M^2 \leq 5$) circular output beam. Current maximum cw output power values for a laboratory setup OPSDL stand as high as 5 W at a heat sink temperature of -15 °C (3 W at 15 °C) for a lasing wavelength of 2 µm [3], and 3.4 W at -10 °C (1.6 W at 20 °C) at a lasing wavelength of 2.25 µm [4]. Furthermore, up-scaling of the output power of mid-infrared OPSDL by using multiple gain elements in a single resonator has also been demonstrated, yielding at 2.25 µm a maximum output power of 3.4 W @ 20 °C for a dual-chip OPSDL [5].

For the wavelength range > 4 µm quantum cascade (QC) lasers are the best suited semiconductor laser variant at present, delivering at room-temperature output powers exceeding the 1 W level with a high-quality ($M^2 < 2$), even though strongly divergent, output beam [6,7]. Current record value for 4.6 µm emitting QC lasers is a maximum room-temperature cw output power of 3.4 W in a laboratory setup [8]. Attempts to further increase the output power have been made (a) by increasing the emitting aperture width of a single emitter from typically ~10 µm to 100 µm, while employing a photonic crystal distributed feedback structure for maintaining a high beam quality, [9] and (b) by combining the output power of several narrow emitters located side-by-side on a single semiconductor chip in an external cavity (EC) setup (spectral beam combining) [10].

While all the above cited characteristics refer to laboratory data, we report in the present paper on the realization of compact infrared laser modules, which cover the 2-2.5 µm and 4.5-5 µm atmospheric transmission windows employing OPSDL and EC-QC laser technology, respectively.

Technologies for Optical Countermeasures VI, edited by David H. Titterton, Mark A. Richardson,
Proc. of SPIE Vol. 7483, 74830F · © 2009 SPIE · CCC code: 0277-786X/09/$18 · doi: 10.1117/12.830342

2. OPSDL MODULE EMITTING AT 2.25 µm

The basic layout of an OPSDL is shown in Fig. 1. The OPSDL chip is an epitaxially grown heterostructure consisting of a semiconductor-based distributed Bragg reflector (DBR), which acts as a planar highly reflective end mirror of the OPSDL cavity, and a semiconductor active region grown on top of the DBR. The active region consists of thin layers of semiconductor material with a smaller energy gap, so called quantum wells (QWs), which are embedded between barrier layers of a wider bandgap semiconductor. The QWs are appropriately placed at the antinodes of the optical standing wave formed in the semiconductor heterostructure. The barrier layers separating the QWs act simultaneously as pump absorbing layers. The DBR is composed of alternating quarter-wave GaSb and AlAsSb layers while the QW layers consist of GaInAsSb and the barrier and pump absorbing layers of AlGaAsSb. The linear OPSDL cavity is terminated by an external concave output coupling mirror. The active region is optically pumped by a fiber-coupled 980 nm emitting diode laser module. The pump light transmitted through the fiber is focused onto the OPSDL chip by appropriate focusing optics, resulting in a pump spot on the chip surface with a diameter of a few hundreds of microns. The transversal mode pattern of the OPSDL is determined by the interplay of the pump spot diameter and the cavity mode diameter on the OPSDL chip. If both are properly matched, a nearly diffraction-limited output beam can be achieved [2].

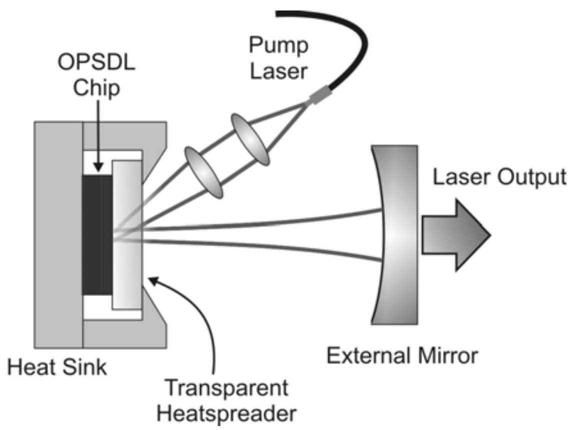

Fig. 1: Schematic OPSDL set-up, composed of the actual OPSDL semiconductor chip, which contains both the gain region and a distributed Bragg reflector (DBR) as the end mirror, and a curved external out-coupling mirror.

Fig. 2: Photograph of a compact 2 µm emitting OPSDL cavity. The approx. dimensions are 80 mm x 30 mm x 50 mm (L x W x H). Optical pumping is achieved by a fiber coupled 980 nm diode laser module (not shown).

Fig. 2 shows a photograph of an actual OPSDL cavity fabricated according to the above linear resonator design. The OPSDL chip, bonded to a SiC intra-cavity heat spreader for an efficient heat extraction from the optically pumped active region, can be seen to the left underneath the ring shaped brass mount. Thermoelectric (TE) cooling is applied for temperature stabilization of the OPSDL chip / SiC heat spreader sandwich. The output beam is emitted through the output coupling mirror to the right. Optical pumping is via an optical fiber entering the cavity from the top right.

Fig. 3 displays a 3D CAD drawing of the portable OPSDL module, containing in its center the above described OPSDL cavity (see Fig. 2) as well as a beam splitter and photo detector for in-line power monitoring. A large finned heat sink for forced air cooling is attached to the rear right of the hermetically sealed inner housing. The OPSDL output beam is emitted towards the front left. Fig. 4 shows a photograph of the completed OPSDL module enclosed by an outer housing for increased robustness and ruggedness. Electrical connections as well as the optical fiber delivering the 980 nm pump light are fed into the module via the corrugated tube seen in the foreground. Laser emission is towards the front.

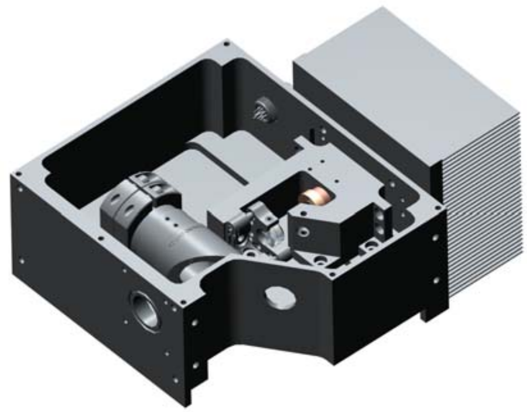

Fig. 3: 3D CAD drawing of the portable OPSDL module.

Fig. 4: Photograph of the portable OPSDL module enclosed by an outer housing.

The cw and pulsed mode output power vs. pump power characteristics of the above OPSDL module are plotted in Fig. 5, while Fig. 6 displays its multiple longitudinal mode lasing spectrum close to the intended wavelength of 2.25 µm. The mode spacing is determined by the optical thickness of the intra-cavity heat spreader acting as an Etalon. The maximum cw output power is 1.25 W at a heat sink temperature of 20 °C, limited by thermal rollover. The maximum low duty cycle pulsed output power exceeds 2.5 W, limited this time by the available pump power rather than by thermal effects. These data clearly demonstrate that, making use of the GaSb-based OPSDL technology, practical 1 W class laser modules can be realized, covering the 2-2.5 µm wavelength band. With the OPSDL module being a cw laser source, also any arbitrary pulse code with modulation frequencies ≥ 10 kHz can be generated simply by on-off modulating the drive current of the 980 nm pump diode lasers.

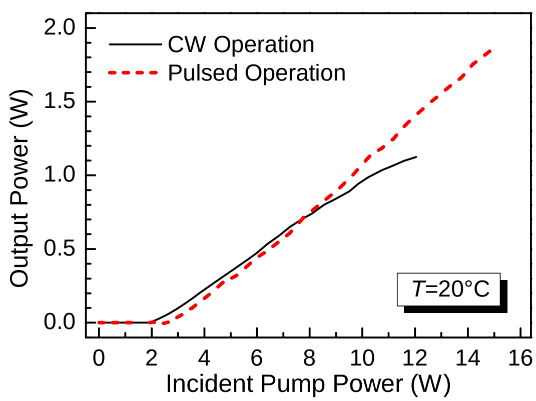

Fig. 5: Continuous-wave (cw) and low duty cycle pulsed mode output power vs. absorbed pump power recorded from the portable 2.25 µm emitting OPSDL module shown in Figs. 3 and 4.

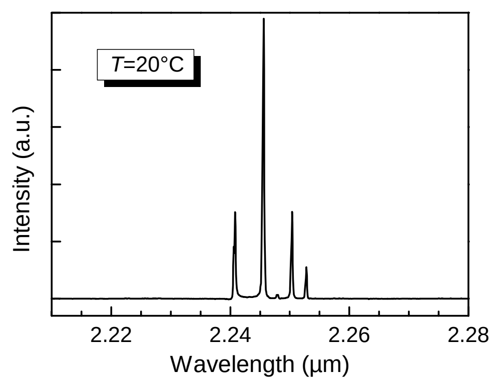

Fig. 6: Continuous wave (cw) lasing spectrum of the portable OPSDL module shown in Figs. 3 and 4.

3. EC-QC LASER MODULE EMITTING AT 4.5-5 µm

Temperature-dependent output power vs. current and total power efficiency vs. current characteristics of a 4.8 µm emitting GaInAs/AlInAs/InP QC laser, designed for high-power operation [11], are displayed in Fig. 7 and 8, respectively. The QC laser test chip, mounted epitaxial-side up on a gold-coated copper submount with the laser facets left uncoated, was operated in low duty-cycle short-pulse mode (100 ns pulses at a repetition rate of 1 kHz) in order to minimize self-heating effects. The maximum single-ended output power, i.e. output power per facet emitted in a collimated beam, amounts to 3.6 W at a heat sink temperature of 270 K and 3 W at 300 K. The corresponding total power efficiency, counting the output power emitted from both facets, is 11.4% at 270 K and still 9.5% at 300 K.

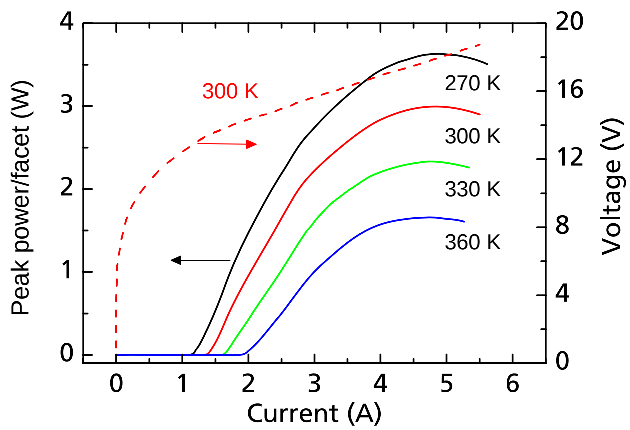

Fig. 7: Temperature-dependent output power-vs.-current characteristics of a 4.8 µm emitting QC laser in pulsed mode operation. The 300 K voltage-current-characteristic is also shown. Ridge width and cavity length are 15 µm and 3 mm, respectively.

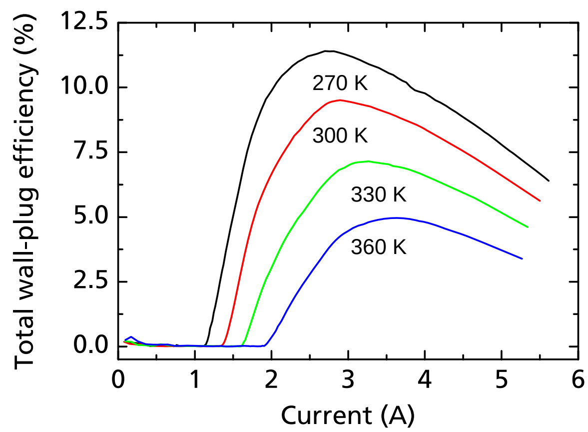

Fig. 8: Temperature-dependent total power efficiency-vs.-current characteristics of a 4.8 µm emitting QC laser in pulsed mode operation. Ridge width and cavity length are 15 µm and 3 mm, respectively.

In spite of the multiple Watt peak output power achieved in **low duty cycle** pulsed mode operation, maximum average output power in **high duty cycle** pulsed mode operation and, even more so, maximum cw output power are still severely limited by thermal effects [9]. This is due to the fact that even in the most favorable situation the vast majority of the injected electrical power is still converted into heat, resulting in strong self-heating of the QC laser active region. As, on the other hand, the power efficiency is strongly temperature dependent, decreasing e.g. to 50% of its initial value when the temperature is raised from 300 K to 360 K (see Fig. 8), thermal runaway of the device active region is a likely scenario unless extreme precautions have been taken to ensure an optimized heat extraction and thermal management.

Therefore, to serve applications like DIRCM which require a high average output power in high duty cycle operation mode, various approaches have been taken towards an efficient combining of the output beams of several individual QC lasers. In this context, an important issue is to preserve the high beam quality delivered by a single narrow ridge waveguide QC laser. As a first approach, beam combining of the output of two QC lasers via polarization coupling has been demonstrated, yielding a maximum coupling efficiency of 82% [12]. A serious drawback of this approach is, however, that it is limited two just two emitters.

To overcome this limitation, the concept of spectral beam combining using an external cavity configuration has been applied to QC lasers, demonstrating the coupling of the output beams of up to 8 individual QC laser ridges, located side-by-side on a single semiconductor chip [10]. Fig. 9 shows a schematic of the EC-QC laser configuration employed here for spectral beam combining of 4.5-5 µm emitting QC lasers [10]. The parallel output beams emitted by the individual

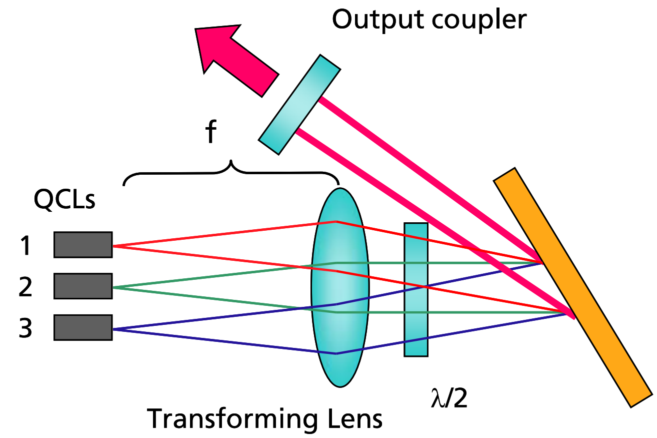

Fig. 9: Schematic of the multiple-emitter EC-QC laser setup employed for spectral beam combining.

QC lasers are collimated by a single custom made aspheric lens (transforming lens) and then directed onto a ruled grating with a blaze angle matched to the operating wavelength of the QC lasers. The different lateral positions of the different emitting apertures are converted by the collimating lens into different angles of incidence on the grating. Adding a partially reflecting planar out-coupling mirror to the setup spectrally selective feedback is provided, which translates the different angles of incidence into different lasing wavelengths for each emitter. On the other hand, the output beam emitted through the planar cavity end mirror is a collinear superposition of the output beams of all emitters, with each emitter lasing at its specific wavelength defined by its lateral position on the chip, the focal length of the transforming lens, as well as the dispersion and angular position of the grating.

Fig. 10 shows the lasing spectrum of such a multiple-emitter EC-QC laser setup, coupling the output of in total 6 individual emitters into a single collimated output beam. The spectrum consists of 6 single lasing modes, equally spaced in wavelength, which proves that all 6 QC lasers are coupled to the external cavity. The combined output beam, on the other hand, is indeed collinear with the original beam quality of a single QC laser well preserved (see the two-dimensional far-field intensity plot in the inset of Fig. 10). Actual beam propagation measurements of the slightly elliptical output beam yield for both the fast and the slow axis M^2 values of < 2. Fig. 11 displays the output power vs. current per emitter characteristics of the multiple-emitter EC-QC laser setup and, for reference purposes, the power vs. current characteristic for a single uncoated Fabry-Perot laser. Both the EC-QC laser and the single device were operated in short-pulse high duty cycle mode, optimized for maximum average output power of the EC-QC laser. There is a threefold increase in average power for the collimated output beam of the EC-QC laser setup as compared to the output of the single emitter (summing up the output power emitted from both facets). Taking into account the total number of emitters coupled, the coupling efficiency can be estimated to 50%. The resulting coupling losses of also 50% are due to cavity losses caused by the finite efficiency of the grating and optical feedback into the emitters via the transforming lens, enforced lasing at wavelengths away from the gain maximum in particular for the emitters located towards both ends of the array, as well as the detrimental effect of increased self-heating due to thermal crosstalk in the multiple emitter chip in the EC-QC laser setup. To suppress the latter effect, the coupling efficiency was also determined for low duty cycle operation, yielding an increased efficiency of 60%. This value constitutes the true optical coupling efficiency of the multiple-emitter EC-QC laser setup. The difference to the former value of 50% for high average power operation confirms that thermal crosstalk between the different laser ridges on the multiple emitter array does indeed play a significant role.

Based on these experiments, a compact beam-combining EC-QC laser module has been designed and fabricated, including all necessary drive and control electronics for short-pulse high duty cycle (≥ 1 MHz repetition rate) operation of a multiple-emitter QC laser chip. Fig. 12 shows a photograph of the EC-QC laser head, which contains also the high frequency drive electronics for the QC lasers. Pulse code modulation at frequencies ≥ 10 kHz is readily achieved by electronically gating the high frequency pulse drain. Due to the high oversampling rate (1 MHz vs. 10 kHz) any pulse shape and sequence can be synthesized with high fidelity.

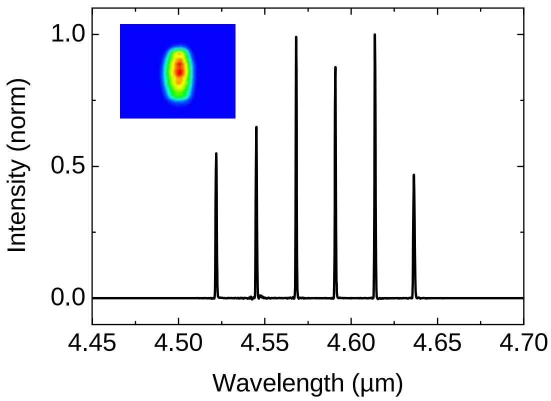

Fig. 10: Lasing spectrum of the multiple-emitter EC-QC laser setup with the power output of 6 QC lasers combined. The inset shows a two-dimensional far-field intensity plot.

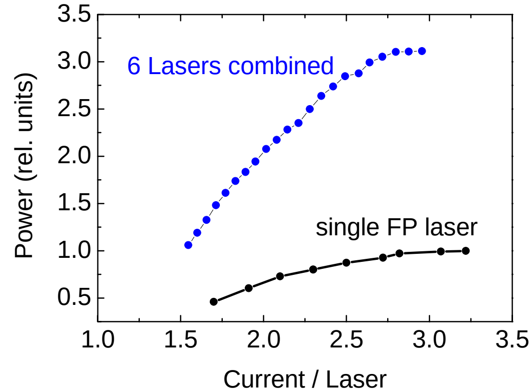

Fig. 11: Output power vs. current per laser characteristics of (a) the multiple-emitter EC-QC laser setup and (b), for reference purposes, the total power emitted from both facets of a nominally identical, uncoated single Fabry-Perot QC laser.

Fig. 12: Portable spectral beam combining EC-QC laser module employing a multiple-emitter laser chip as the light engine.

4. SUMMARY

In conclusion, compact and robust infrared semiconductor laser modules have been realized, which cover the 2-2.5 µm and 4.5-5 µm wavelength bands employing OPSDL and QC laser technology in conjunction with spectral beam combining, respectively. These modules meet both in terms of wavelength coverage, output power and beam quality as well as in terms of pulse code modulation capability initial specifications for a semiconductor laser based DIRCM system. These modules are ready for use in corresponding field trials to explore the potential of (quasi-)cw semiconductor laser technology for deception class DIRCM.

ACKNOWLEDGEMENTS

The authors would like to thank R. Lösch, T. Lüdke, A. Michailov, R. Moritz, O. Neumaier, K. Schäuble, K. Schwarz, and U. Weinberg for expert technical assistance. Financial support by the German Ministry of Defence is gratefully acknowledged.

REFERENCES

[1] D. H. Titterton, "Development of infrared countermeasure technology and systems", in „Mid-infrared Semiconductor Optoelectronic", ed. A. Krier (Springer, Heidelberg, 2005), p. 635.

[2] N. Schulz, J.-M. Hopkins, M. Rattunde, D. Burns, and J. Wagner, "High-brightness long-wavelength semiconductor disk lasers", Laser & Photon. Rev. 2, 160 (2008).

[3] J.-M. Hopkins, N. Hempler, B. Rösener, N. Schulz, M. Rattunde, C. Manz, K. Köhler, J. Wagner, and D. Burns, „High-power, (AlGaIn)(AsSb) semiconductor disk laser at 2.0 µm", Opt. Lett. 33, 201 (2008).

[4] B. Rösener, N. Schulz, M. Rattunde, C. Manz, K. Köhler, and J. Wagner, „High-Power, High-Brightness Operation of a 2.25µm (AlGaIn)(AsSb)-based Barrier-pumped Vertical-External-Cavity Surface-Emitting Laser", IEEE Photon. Technol. Lett. 20, 502 (2008).

[5] B. Rösener, M. Rattunde, R. Moser, C. Manz, K. Köhler, and J. Wagner, „GaSb-based optically pumped semiconductor disk laser using multiple gain elements", IEEE Photon. Technol. Lett. 21, 848 (2009).

[6] A. Lyakh, C. Pflügl, L. Diehl, Q. J. Wang, F. Capasso, X. J. Wang, J. Y. Fan, T. Tanbun-Ek, R. Maulini, A. Tsekoun, R. Go, and C. Kumar N. Patel, "1.6 W high wall plug efficiency, continuous-wave room temperature quantum cascade laser emitting at 4.6 µm", Appl. Phys. Lett. 92, 111110 (2008).

[7] Y. Bai, S. Slivken, S. R. Darvish, and M. Razeghi, " Room temperature continuous wave operation of quantum cascade lasers with 12.5% wall plug efficiency", Appl. Phys. Lett. 93, 021103 (2008).

[8] M. Razeghi, Proc. SPIE 7230, 723011 (2009).

[9] Y. Bai, B. Gokden, S. R. Darvish, S. Slivken, and M. Razeghi, "Photonic crystal distributed feedback quantum cascade lasers with 12 W output power", Appl. Phys. Lett. 95, 031105 (2009).

[10] S. Hugger, F. Fuchs, R. Aidam, W. Bronner, R. Lösch, Q. Yang, N. Schulz, J. Wagner, E. Romasew, M. Raab, and H. D. Tholl, "Spectral beam combining of quantum cascade lasers in an external cavity", Proc. SPIE 7325, 732517 (2009).

[11] Q. Yang, R. Lösch, W. Bronner, S. Hugger, F. Fuchs, R. Aidam, and J. Wagner, „High-peak-power strain-compensated GaInAs/AlInAs quantum cascade lasers (λ~4.6 µm) based on a slightly-diagonal active region design", Appl. Phys. Lett. 93, 251110 (2008).

[12] J. Wagner, N. Schulz, B. Rösener, M. Rattunde, Q. Yang, F. Fuchs, C. Manz, W. Bronner, C. Mann, K. Köhler, M. Raab, E. Romasev, and H. D. Tholl, „Infrared semiconductor lasers for DIRCM applications", Proc. SPIE 7115, 71150A (2008).